

## OBSERVATION OF FURTHER MEYER-NELDEL RULE IN $\text{Se}_{70}\text{Te}_{30-x}\text{Sb}_x$ THIN FILMS

K. SHARMA, M. LAL<sup>a</sup>, A. KUMAR, N. GOYAL\*

*Department of Physics, Panjab University, Chandigarh, India-160014.*

*<sup>a</sup>GGDSD College, Chandigarh, India-160030.*

Temperature dependence of conductivity for amorphous  $\text{Se}_{70}\text{Te}_{30-x}\text{Sb}_x$  thin films is measured in the temperature range 253 - 343 K and in the intensity range 10-1043 Lux. By taking two different approaches, we have investigated Meyer Neldel rule and further Meyer Neldel rule in  $\text{Se}_{70}\text{Te}_{30-x}\text{Sb}_x$  thin films. In the first approach, different sets of pre-exponential factor  $\sigma_0$  and activation energy ( $\Delta E$ ) are obtained at different illumination intensities by keeping composition constant. The pre-exponential factor ( $\sigma_0$ ) is found to be correlated with activation energy ( $\Delta E$ ) following Meyer - Neldel (MN) rule. The observation of further MN rule is also observed in which strong correlation between Meyer Neldel pre-factor  $\sigma_{00}$  and Meyer Neldel energy  $E_{mn}$  is satisfied. In the second approach, different sets of pre-exponential factor  $\sigma_0$  and activation energy ( $\Delta E$ ) are obtained at fixed illumination intensities by changing the composition. Also in the second approach, a strong correlation between Meyer Neldel pre-factor  $\sigma_{00}$  and Meyer Neldel energy  $E_{mn}$  has been observed.

(Received December 15, 2014; Accepted February 7, 2014)

*Keywords:* Photoconductivity, Chalcogenide glasses, Amorphous, Thin films, Activation energy

### 1. Introduction

Chalcogenide glasses have vast electrical, optical and technological applications, such as irreversible phase change based optical recording, memory devices, optical fibers, xerography, photolithography, infrared lenses, optical amplifiers, blue laser diodes and solar cells [1-7]. Erasable recording is usually considered to be a potential replacement for conventional recording due to its high storage density and archival stability. Selenium tellurium based chalcogenides have received particular attention because of their potential for application in electronics [8-9]. Generally, undoped chalcogenide glasses show low electrical conductivity which limits their technological application. Certain additives are used to improve their properties. The interest in these materials arises particularly due to their ease of fabrication in the bulk form and thin films. Furthermore, one can easily change the properties of these glasses by varying their chemical composition (synthesis regime) [10-11] or irradiating them by light (photo induced phenomena) [12-13].

In general, the measurements of d. c. conductivity in case of semiconductor materials have yielded valuable information about the transport mechanism. The majority of semiconductors show activated temperature dependence according to the relation (1),

$$\sigma = \sigma_0 \exp(-\Delta E/kT) \quad (1)$$

where  $\Delta E$  and  $\sigma_0$  are the activation energy and pre-exponential factor respectively.

---

\*Corresponding author: ngoyal@pu.ac.in

The correlation between  $\sigma_0$  and  $\Delta E$  is given by

$$\sigma_0 = \sigma_{00} \exp(\Delta E/E_{MN}) \quad (2)$$

where  $\sigma_{00}$  and  $E_{MN}$  are constants for the system. The above equation is known as Meyer – Neldel (MN) rule [14] which is applicable to various thermally activated phenomena.  $E_{MN} = kT_0$  is called Meyer–Neldel characteristic energy and  $\sigma_{00}$  is MN pre-factor. Recently, Meyer-Neldel rule has been found to be applicable to thermally activated phenomenon like d. c. conduction and a. c. conduction in chalcogenide glasses [15-20], in many organic solids [21] and even in ionically conducting crystals and glasses [22].

Thus, the observation of Meyer- Neldel rule in various thermally activated phenomena for different material is well known. Shimakawa and Abdel-Waheb [15] also found a strong correlation between  $\sigma_{00}$  and  $E_{MN}$

$$\ln \sigma_{00} = A + B E_{MN} \quad (3)$$

where A and B are constants. This relation between the Meyer-Neldel pre-factor  $\sigma_{00}$  and Mayer Neldel energy  $E_{MN}$  is known as further Meyer-Neldel rule.

Keeping this in mind, we have studied the effect of Antimony impurity on photo induced phenomena in  $\text{Se}_{70}\text{Te}_{30}$  and report the evidence of Meyer-Neldel rule and further Meyer-Neldel rule in  $\text{Se}_{70}\text{Te}_{30-x}\text{Sb}_x$  ( $x = 0, 2, 4, 6, 8$ ) thin films by taking two approaches. In first approach,  $\sigma_{00}$  is obtained at different illumination intensities from temperature dependence of conductivity and tried to investigate whether there is a correlation or not between Meyer Neldel conductivity pre-factor  $\sigma_{00}$  and the characteristic energy  $E_{MN}$  in Se-Te-Sb glassy system. In second approach, we have tried to investigate, whether there is a correlation or not between Meyer Neldel conductivity pre-factor  $\sigma_{00}$  and the characteristic energy  $E_{MN} = kT_0$  by varying the composition of the glassy system.

## 2. Experimental procedure

Glassy alloys of  $\text{Se}_{70}\text{Te}_{30-x}\text{Sb}_x$  ( $x = 0, 2, 4, 6, 8$ ) were prepared by melt-quench technique. High purity 99.999% Bi, Sb and Te granules were weighted according to the formula of  $\text{Se}_{70}\text{Te}_{30-x}\text{Sb}_x$  ( $x = 0, 2, 4, 6, 8$ ). The powder mixture was loaded into quartz ampoule and sealed under vacuum at  $10^{-4}$  Pa. The sealed quartz ampoule was loaded in a furnace and heated to  $950^\circ\text{C}$  at a rate of  $3\text{-}4^\circ\text{C}/\text{minute}$  for 18 hours to ensure the composition homogeneity and quenched in liquid nitrogen. The ingots were crushed, separated, grounded and characterized. The glassy nature of alloys was checked by X-ray diffraction technique.

The thin films were synthesized by thermal evaporation technique under high vacuum conditions ( $\sim 10^{-4}$  Pa) using a small piece of bulk alloy as a source material and glass as a substrate. For electrical measurements vacuum – evaporated indium electrodes were used. A coplanar structure (length  $\sim 1.8$  cm and separation between electrodes  $\sim 0.7$  mm) was used for present measurements.

A three terminal sample holder in which light could be shown through a transparent window has been used for the measurement of steady state photoconductivity of thin films. A copper- constantan thermocouple has been inserted inside the sample holder and kept close to the sample to measure the correct temperature. A vacuum of the order of  $10^{-4}$  to  $10^{-5}$  Torr was achieved inside the sample holder using vacuum pump. The light source for these measurements was a 200 W tungsten lamp. Before measurement, the films were first annealed at their glass transition temperature for two hours in a vacuum  $\sim 10^{-4}$  Torr. The present measurements were made by applying only 10 V across the films using dc power supply (CROWN DC-regulated Power Supply 0-30V/2A) and the resulting current was measured with digital piccoammeter (Digital Piccoammeter DPM-111, Scientific equipment Roorkee).

### 3. Result and discussion

For amorphous thin films, the temperature dependence of photoconductivity at different intensities was studied in the temperature range 253-343 K and results are shown in Figs. 1-5. From all figures, it is clear that at each intensity,  $\ln \sigma_{ph}$  and  $1000/T$  plots are straight lines in the observed temperature range and photoconductivity is an activated process with single activation energy. This type of behavior is consistent with Eq. (1). The activation energy ( $\Delta E$ ) is determined from the slope of the straight lines in the resulting plots at different intensities and curve fitting is done by least square method. The intercepts of the lines give the value of  $\ln \sigma_0$ . For  $Se_{70}Te_{30-x}Sb_x$  ( $x = 0, 2, 4, 6, 8$ ) amorphous thin films, the value of  $\Delta E$  and  $\ln \sigma_0$  are given in Table 1-5.

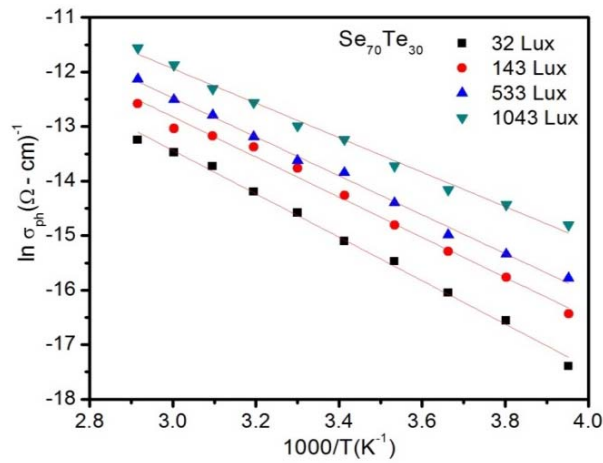


Fig.1.  $\ln \sigma_{ph}$  vs  $1000/T$  for amorphous  $Se_{70}Te_{30}$  thin film at different illumination intensities.

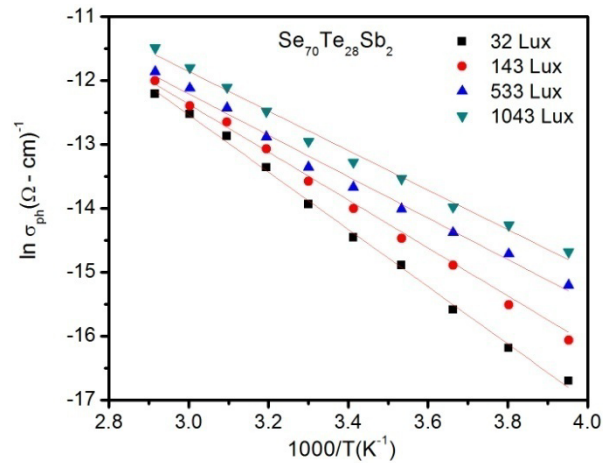


Fig.2.  $\ln \sigma_{ph}$  vs  $1000/T$  for amorphous  $Se_{70}Te_{28}Sb_2$  thin film at different illumination intensities.

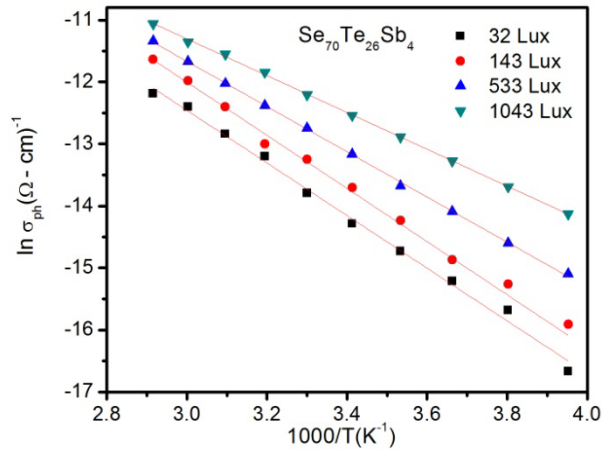


Fig. 3.  $\ln \sigma_{ph}$  vs  $1000/T$  for amorphous  $Se_{70}Te_{26}Sb_4$  thin film at different illumination intensities.

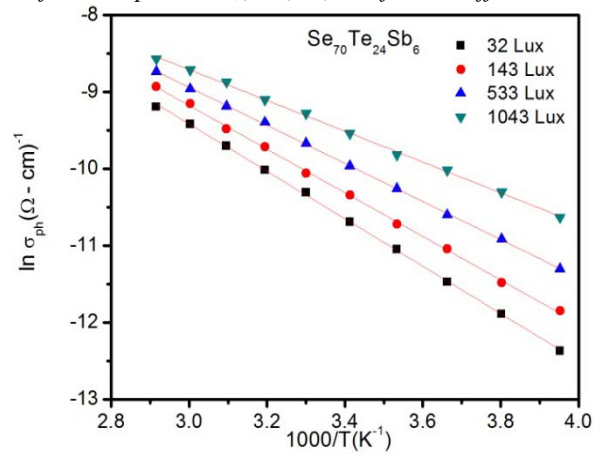


Fig. 4.  $\ln \sigma_{ph}$  vs  $1000/T$  for amorphous  $Se_{70}Te_{24}Sb_6$  thin film at different illumination intensities.

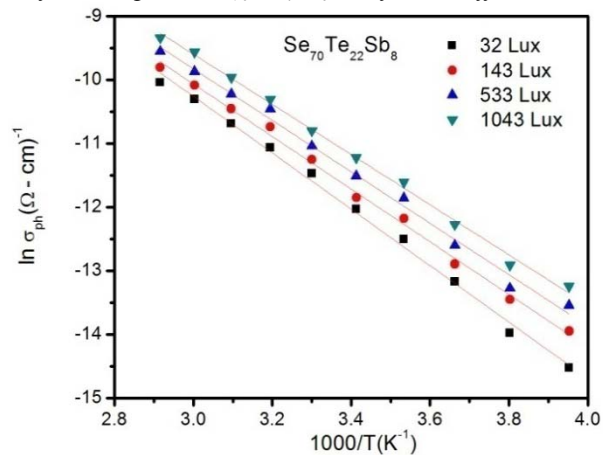


Fig. 5.  $\ln \sigma_{ph}$  vs  $1000/T$  for amorphous  $Se_{70}Te_{22}Sb_8$  thin film at different illumination intensities.

It is evident from Figs. 1-5 and from Tables 1-5 that for each sample, the conductivity increases and activation energy decreases with increase of the light intensity, indicating shift of Fermi level with intensities. The Fermi level split into quasi Fermi levels in the presence of light and moves toward the valance band for holes and toward the conduction band for electrons [23]. The position of these quasi Fermi levels depends on the light intensity and activation energy therefore become smaller. Here we also observed that at each intensity, as Sb composition

increases upto 6% in alloys, conductivity continues to increase. With further increase of Sb composition (when  $x=8$ ) in alloy conductivity decreases. This can be explained in terms of electron affinity of constituent elements [24]. When Te is added to Se, some of the Te atoms may not be incorporated in chains and act as ionized impurities (electron affinity of Te (1.97 eV) is lower than that of Se (2.02 eV)). The electron affinity of Sb (1.07 eV) is much lower than that of both Se and Te and addition of Sb will induce more and more positively charged localized states and hence defect states increases. So increase in defect state density after incorporating Sb additive in various concentrations to binary  $\text{Se}_{70}\text{Te}_{30}$  alloy may be understood in terms of lower electron affinity of Sb as compared to Se and Te. When concentration of Sb is further increased, the system becomes more disordered and density of localized states decreases which leads to decrease in conductivity of  $\text{Se}_{70}\text{Te}_{22}\text{Sb}_8$  as compared to  $\text{Se}_{70}\text{Te}_{24}\text{Sb}_6$  [25].

*Table 1: Values of activation energy ( $\Delta E$ ) and pre-exponential factor for  $\text{Se}_{70}\text{Te}_{30}$  thin film at various intensity (first approach)*

F (LUX)	$\Delta E$ (eV)	$\ln \sigma_0$ ( $\Omega\text{-cm}$ ) <sup>-1</sup>
32	0.343	-1.094
143	0.317	-1.779
533	0.307	-1.823
1043	0.272	-2.448

*Table 2: Values of activation energy ( $\Delta E$ ) and pre-exponential factor for  $\text{Se}_{70}\text{Te}_{28}\text{Sb}_2$  thin film at various intensity (first approach)*

F (LUX)	$\Delta E$ (eV)	$\ln \sigma_0$ ( $\Omega\text{-cm}$ ) <sup>-1</sup>
32	0.387	0.9258
143	0.324	-1.1117
533	0.279	-2.4727
1043	0.267	-2.5641

*Table 3: Values of activation energy ( $\Delta E$ ) and pre-exponential factor for  $\text{Se}_{70}\text{Te}_{26}\text{Sb}_4$  thin film at various intensity (first approach)*

F (LUX)	$\Delta E$ (eV)	$\ln \sigma_0$ ( $\Omega\text{-cm}$ ) <sup>-1</sup>
32	0.3697	0.8667
143	0.3461	0.2855
533	0.3146	-0.7225
1043	0.2562	-2.3918

*Table 4: Values of activation energy ( $\Delta E$ ) and pre-exponential factor for  $\text{Se}_{70}\text{Te}_{24}\text{Sb}_6$  thin film at various intensity (first approach)*

F (LUX)	$\Delta E$ (eV)	$\ln \sigma_0$ ( $\Omega\text{-cm}$ ) <sup>-1</sup>
32	0.2662	-0.1551
143	0.2449	-0.6571
533	0.2137	-1.5036
1043	0.1731	-2.6882

Table 5: Values of activation energy ( $\Delta E$ ) and pre-exponential factor for  $Se_{70}Te_{22}Sb_8$  thin film at various intensity (first approach)

F (LUX)	$\Delta E$ (eV)	$\ln \sigma_0 (\Omega\text{-cm})^{-1}$
32	0.3827	3.0552
143	0.3568	2.3497
533	0.3491	2.3169
1043	0.3402	2.2415

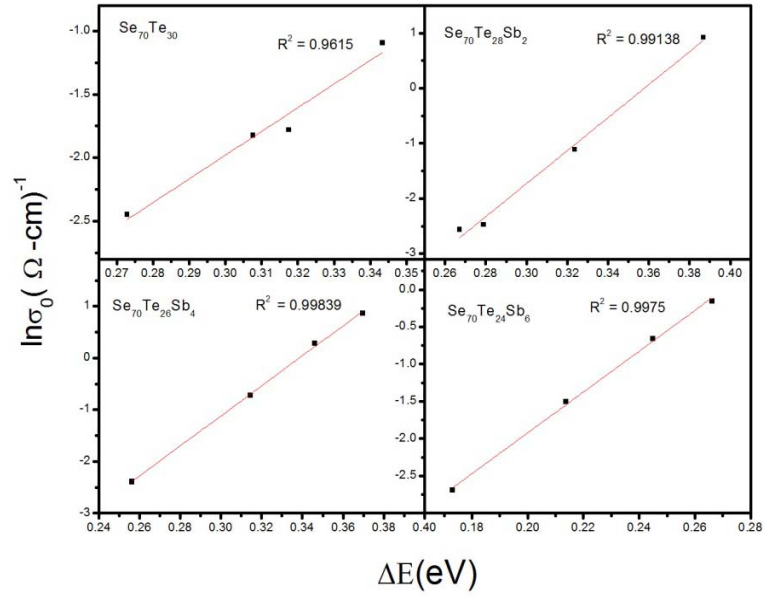


Fig.6.  $\ln \sigma_0$  vs  $\Delta E$  for amorphous  $Se_{70}Te_{30-x}Sb_x$  ( $0 \leq x \leq 6$ ) thin films according to first approach.

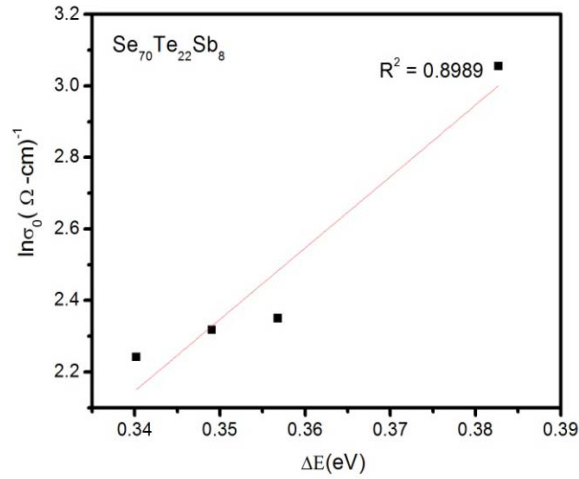


Fig.7. According to first approach,  $\ln \sigma_0$  vs  $\Delta E$  for amorphous  $Se_{70}Te_{22}Sb_8$  thin film.

Table 6: According to First approach,  $\ln \sigma_{00}$  and  $E_{MN} = kT_0$  for amorphous  $Se_{70}Te_{30-x}Sb_x$  ( $0 \leq x \leq 8$ ) thin films

Series	$E_{MN} = kT_0$ (eV)	$\ln \sigma_{00} (\Omega\text{-cm})^{-1}$
x = 0	0.0534	-7.589
x = 2	0.0334	-10.706
x = 4	0.0344	-9.832
x = 6	0.0366	-7.387
x = 8	0.0502	-4.651

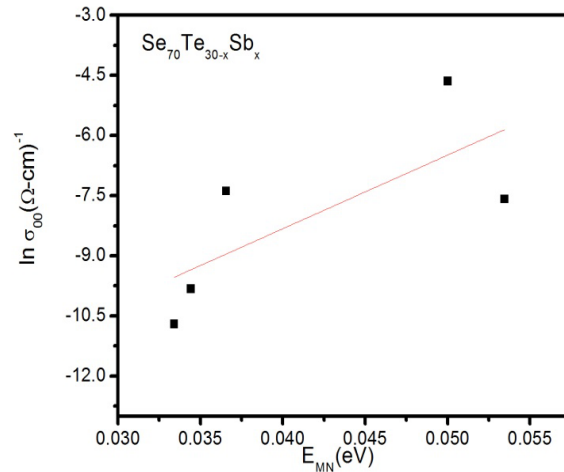


Fig.8.  $\ln \sigma_{00}$  vs  $E_{MN} = kT_0$  for amorphous  $\text{Se}_{70}\text{Te}_{30-x}\text{Sb}_x$  ( $0 \leq x \leq 8$ ) thin films according to first approach

According to first approach, the plots of  $\ln \sigma_0$  and  $\Delta E$  for  $\text{Se}_{70}\text{Te}_{30-x}\text{Sb}_x$  are shown in Fig. 6-7 and which are straight lines indicating that  $\sigma_0$  varies exponentially with  $\Delta E$  following the relation as given in Equation (2). From Table 6, it is clear that the value of Meyer Neldel conductivity pre-factor  $\sigma_{00}$  (calculated from intercepts of the plots of  $\ln \sigma_0$  and  $\Delta E$ ) is different at different compositions. Also it is interesting to note that the value of characteristic energy  $E_{MN} = kT_0$  (calculated from slopes of the plots of  $\ln \sigma_0$  and  $\Delta E$ ) is also different at different compositions. When we plot  $\ln \sigma_{00}$  as a function of  $E_{MN} = kT_0$ , a straight line is obtained as shown in Fig. 8. Fig. 8 indicates a strong correlation between  $\sigma_{00}$  and  $E_{MN} = kT_0$  and can be describing the following relation (4) which is proposed by Shimakawa and Abdel-Waheb [15]:

$$\sigma_{00} = \sigma'_{00} \exp(kT_0/\varepsilon) \quad (4)$$

where  $\varepsilon$  is a constant.

Banik [26] explained the further Meyer Neldel rule on the basis of barrier cluster model. According to Banik the “further MNR” takes into account the fact that the during recombination process equi-energy phonons will be produced and these phonons will be absorbed by free electrons in the low mobility sub-band. The transport of electrons near lower band edge takes place via tunneling across potential energy barriers. The electrons are excited to higher energy levels when phonons are absorbed and which implies a considerable electrical conductivity enhancement. This enhancement corresponds with the empirical relation known as the further Mayer Neldel rule as given in equation (3). Shimakawa and Abdel-Waheb [15] have reported the strong correlation between  $\sigma_{00}$  and  $kT_0$  in case of chalcogenide glasses and is called as further MN rule. In their case,  $\varepsilon$  has a value 1.7 meV. Yelon and Movaghar [27-28] explained the correlation between MN pre-factor  $\sigma_{00}$  and MN energy by multiple excitations stimulated by optical phonon energy. Crandall [29] and Chen [30] explained a correct description of the MN conductivity pre-factor for  $\text{C}_{60}$  films. Wang and Chen [31] have also shown that the conductivity in fullerenes obeys the Meyer-Neldel rule and also found that the correlation between  $\sigma_{00}$  and  $kT_0$  exists. Ashok Kumar [32-33] explained the strong correlation between  $\sigma_{00}$  and  $kT_0$  with a. c. conduction in bulk glassy  $\text{Se}_{70}\text{Te}_{30-x}\text{Zn}_x$  alloys as well as for photoconductive  $\text{Se}_{70}\text{Te}_{30-x}\text{Zn}_x$  thin films.

Table 7: Values of activation energy and pre-exponential factor for  $Se_{70}Te_{30-x}Sb_x$  thin films at 32 Lux (second approach).

Series	$\Delta E$ (eV)	$\ln \sigma_0 (\Omega\text{-cm})^{-1}$
0	0.3979	1.2897
2	0.3859	1.1132
4	0.3827	0.9965
6	0.3434	-0.7936
8	0.2862	-1.1151

Table 8: Values of activation energy and pre-exponential factor for  $Se_{70}Te_{30-x}Sb_x$  thin films at 143 Lux (second approach)

Series	$\Delta E$ (eV)	$\ln \sigma_0 (\Omega\text{-cm})^{-1}$
0	0.3699	0.2276
2	0.3568	0.0997
4	0.3236	-0.8212
6	0.2975	-1.6817
8	0.3149	-1.2707

Table 9: Values of activation energy and pre-exponential factor for  $Se_{70}Te_{30-x}Sb_x$  thin films at 533Lux (second approach)

Series	$\Delta E$ (eV)	$\ln \sigma_0 (\Omega\text{-cm})^{-1}$
0	0.3291	0.4169
2	0.3142	-0.7225
4	0.2976	-1.431
6	0.2678	-1.676
8	0.2831	-1.372

Table 10: Values of activation energy and pre-exponential factor for  $Se_{70}Te_{30-x}Sb_x$  thin films at 1043 Lux (second approach)

Series	$\Delta E$ (eV)	$\ln \sigma_0 (\Omega\text{-cm})^{-1}$
0	0.3125	-1.878
2	0.3097	-2.413
4	0.2876	-3.291
6	0.2462	-3.928
8	0.2731	-3.713

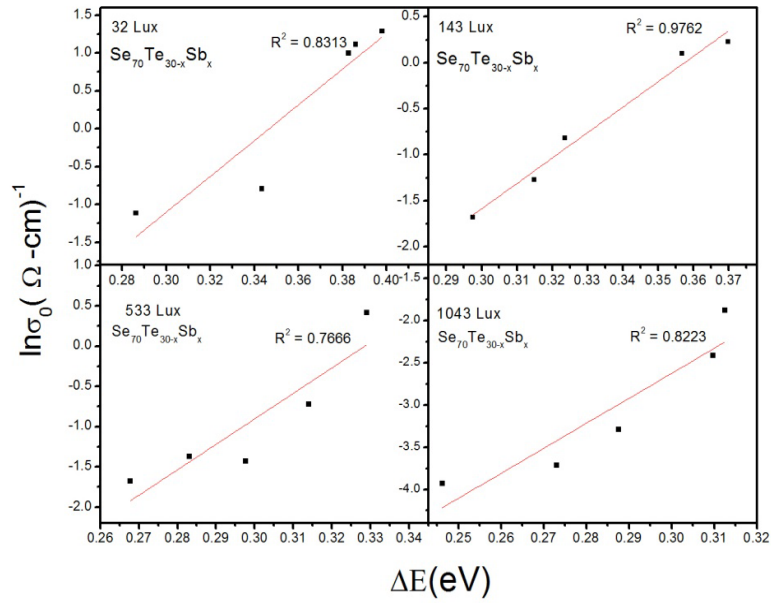


Fig.9. For the second approach,  $\ln\sigma_0$  vs  $\Delta E$  for amorphous  $Se_{70}Te_{30-x}Sb_x$  ( $0 \leq x \leq 6$ ) thin films ( $x$  as a variable).

Table 11: According to second approach,  $\ln\sigma_{00}$  vs  $E_{MN} = kT_0$  for amorphous  $Se_{70}Te_{30-x}Sb_x$  ( $0 \leq x \leq 8$ ) thin films (different composition with illumination as variable)

F(Lux)	$E_{MN} = kT_0$ (eV)	$\ln \sigma_{00} (\Omega\text{-cm})^{-1}$
32	0.0423	-8.1839
143	0.0362	-9.8821
513	0.0315	-10.4016
1043	0.0338	-11.6851

In the second approach, for different compositions  $\Delta E$  and  $\sigma_0$  are observed at a particular intensity and plotted in Fig. 9 and values are given in Table 7-10. At different intensities, the values of  $kT_0$  and  $\sigma_{00}$  are calculated from the slopes and intercepts of these curves and given in Table 11. On plotting  $\ln \sigma_{00}$  as function of  $E_{MN} = kT_0$ , a straight line is obtained as shown in Fig. 10. A strong correlation exists between  $\sigma_{00}$  and  $E_{MN} = kT_0$  in this approach also.

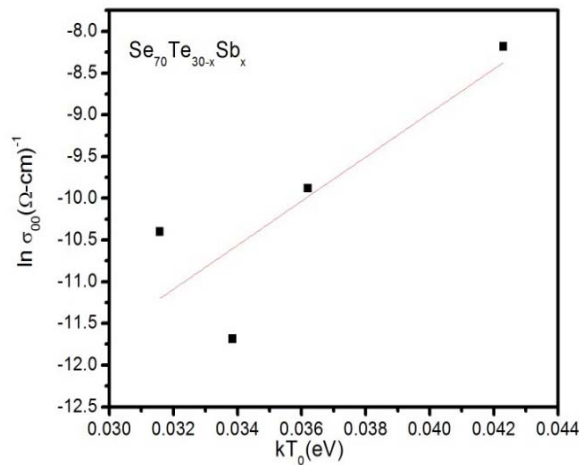


Fig.10.  $\ln\sigma_{00}$  vs  $E_{MN} = kT_0$  for amorphous  $Se_{70}Te_{30-x}Sb_x$  ( $0 \leq x \leq 8$ ) thin films according to second approach

From the above described facts, we have tried to investigate whether the set of values of  $\sigma_{00}$  and  $kT_0$  obtained in our case for  $\text{Se}_{70}\text{Te}_{30-x}\text{Sb}_x$  ( $0 \leq x \leq 8$ ) thin films can be fitted or not in Eq. (4). This is found true in the present case for both the approaches. In first approach,  $\ln\sigma'_{00} = -15.668$  and  $\varepsilon = 0.00544$  meV and in second approach,  $\ln\sigma'_{00} = -19.534$  and  $\varepsilon = 0.00378$  meV. The values are close to the range suggested by Shimakawa and Abdel-Waheb [15] for chalcogenide glasses.

#### 4. Conclusion

Two set of data are collected to observe the presence of Meyer Neldel rule and further Meyer Neldel in  $\text{Se}_{70}\text{Te}_{30-x}\text{Sb}_x$  ( $0 \leq x \leq 8$ ) thin films. In first approach, for a particular amorphous thin film, variation of activation energy is observed at different intensities and also the activation energy of photoconduction decreases with increase in the intensity which indicates illumination causes a shift in the Fermi level due to splitting of the Fermi level into quasi Fermi levels. For all glassy alloys, the pre-exponential factor  $\sigma_0$  shows correlation with activation energy  $\Delta E$  following the Meyer-Neldel rule. Also at a fixed intensity of light, the increase of  $\sigma_{ph}$  with Sb corporation indicates an increase in the density of defect state. In second approach, at a fixed intensity of light the variation of activation energy is observed at different compositions. It is found that  $\sigma_0$  varies with  $\Delta E$  in second approach also. In both the cases, a further MN rule is also observed where a correlation between  $\sigma_{00}$  and  $kT_0$  is satisfied. In both approaches, the results of further MN rule are similar those obtained by Shimakawa and Abdel-Waheb in chalcogenide glasses.

#### Reference

- [1] M. Sexsena, S. Gupta, A. Agarwal, Appl. Sci. Reseach **2(2)**, 109-116 (2011).
- [2] G. Kaur, T. Komastu, J. Mater. Sci. **36**, 453 (2001).
- [3] Z. Abdel-Khelek Ali, G. H. Adel, A. S. Abd-rao, Chalc. Lett. **6**, 125 (2009).
- [4] V. Trnovoca, I. Furar, D. Lezal, J. Non-Cryst. Solids **353**, 1311 (2007).
- [5] A. Kumar, P. B. Barman, R. Sharma, adv. Apply. Sci. Research **1(2)**, 47 (2010).
- [6] A. Kumar, M. Lal, K. Sharma, S. K. Tripathi, N. Goyal, Ind. J. Pure and Appl. Phys. **51**, 251 (2012).
- [7] A. Kumar, M. Lal, K. Sharma, S. K. Tripathi, N. Goyal, chalk. Lett. **9**, 275 (2012).
- [8] V. K. Sarawat, V. Kishore, K. Singh, N. S. Sexsena, T. P. Sharma, Chalc. Lett. **3**, 61 (2006).
- [9] R. M. Mehra, G. Kaur, P. C. Mathur, J. Mater. Sci. **26**, 3433 (1991).
- [10] A. A. Manshina, A. V. Kurochkin, S. V. Degtyarev, Ya. G. Grigoriev, A. S. Tverjanovich, Yu. S. Tveryanovich, V. B. Smirnov, Proc. SPIE **4429**, 80 (2001).
- [11] A. S. Tverjanovich, Ya. G. Grigoriev, S. V. Degtyarev, A. V. Kurochkin, A. A. Manshina, Yu. S. Tveryanovich, J. Non-Cryst. Solids **286**, 89 (2001).
- [12] K. Tanaka, K. Ishida, N. Yoshida, Phys. Rev. B **54**, 9190 (1996).
- [13] Ambika, P. B. Barman, Asian J. Chem. **21**, S028-032 (2009).
- [14] W. Meyer, H. Neldel, Z. Tech. Phys. **12**, 588 (1937).
- [15] K. Shimakawa, Abdel-Waheb, Appl. Phys. Lett. **70**, 652 (1997)
- [16] N. Khushwaha, N. Mehta, R. K. Shukla, D. Kumar, A. Kumar, J. Optoelectron. Adv. Mater. **7**, 2293 (2005).
- [17] D. Kumar, S. Kumar, Chalc. Lett. **1**, 79 (2004).
- [18] S. Parkash, K. Kaur, N. Goyal, S. K. Tripathi, Pramana **76**, 629 (2011).
- [19] N. Mehta, Current Opinion in Solid State and Mater. Sci. **14**, 95 (2010).
- [20] M. F. Kotkata, J. Non-Cryst. Solids **358**, 420 (2010).
- [21] B. Rosenberg, B. B. Bhowmik, H. C. Harder, E. Postow, J. Chem. Phys. **49**, 4108 (1968).
- [22] D. P. Almond, G. K. Duncan, A. R. West, J. Non-Cryst. Solids **74**, 285 (1985).
- [23] D. Kumar, S. Kumar, Ind. J. Pure & Appl. Phys. **42**, 771-774 (2004).
- [24] S. K. Tripathi, V. Sharma, A. Thakur, J. Sharma, G. S. S. Saini, N. Goyal, J. Non-Cryst. Solids **351**, 2468-2473 (2005).

- [25] A. Kumar, M. Lal, K. Sharma, S. K. Tripathi, N. Goyal, *J. Non-Oxide Glasses* **5**, 27 (2013).
- [26] Banik, J. *Optoelectron. Adv. Mater.* **12**, 2247-2254 (2010).
- [27] Yelon, B. Movaghar, *Phys. Rev. Lett.*, **65**, 618 (1990).
- [28] A. Yelon, B. Movaghar, H. M. Branz, *Phys. Rev. B*, **46**, 12244 (1992).
- [29] R. S. Crandall, *Phys. Rev. B* **43**, 4057 (1991).
- [30] Y. F. Chen, S. F. Huang, *Phys. Rev. B* **44**, 13 775 (1991).
- [31] J. C. Wang, Y. F. Chen, *Appl. Phys. Lett.* **73**, 948 (1998).
- [32] R. K. Pal, A. K. Agnihotri, P. K. Dwivedi, A. Kumar, *J. Ovn. Research* **5**, 135-144 (2009).
- [33] S. Srivastva, S. Yadav, R. K. Shukla, A. Kumar, *J. Non-Oxide Glasses* **1**, 51-58 (2010).